PHYSICAL REVIEW B VOLUME 15, NUMBER 12 15 JUNE 1977

Self-consistent pseudopotential calculations for the ideal (001) surface of Nb†

Steven G. Louie,* Kai-Ming Ho, James R. Chelikowsky,‡ and Marvin L. Cohen
Department of Physics, University of California, and Materials and Molecular Research Division, Lawrence Berkeley Laboratory, Berkeley, California 94720
(Received 24 January 1977)

A nonlocal self-consistent pseudopotential scheme is employed to calculate the electronic structure of the ideal (001) surface of Nb. Charge densities, electronic local density of states, and the two-dimensional band structure for the surface are presented and discussed. Prominent surface bands and surface resonances are identified and analyzed throughout the two-dimensional Brillouin zone. The projected Nb bulk band structure on the (001) surface is also obtained. Surface states of different angular momentum character are found to exist over a wide range of energies and over different portions of the two-dimensional Brillouin zone. Our calculations predict strong surface features in the density of states in the range 0–2 eV above the Fermi energy.

I. INTRODUCTION

In the last few years, theoretical progress in the understanding of the electronic properties of metal surfaces has lagged behind that of semiconductor surfaces. Simple s-p metal surfaces lack the wealth of interesting experimental data which have attracted the theorists to work on semiconductor surfaces. On the other hand, although transition-metal surfaces are of great interest because of their possible technological applications[1] and of the rapidly growing amount of experimental information gathered,[2] the complexity arising from the d electrons has made realistic calculations on these surfaces prohibitively difficult. Thus far, existing calculations[1,2] on the electronic properties of transition-metal surfaces are rather primitive compared to the work done on semiconductor surfaces[3,4] and none has yet fully incorporated the important effects of the self-consistent rearrangement of the electrons at the surface.

We present in this paper the first such self-consistent calculations on the surface electronic structure of a transition metal. The potential, charge density, and two-dimensional band structure for the ideal (001) surface of niobium is obtained using a self-consistent pseudopotential method.[4,5] We have also calculated a local density of states which displays the density of states (electronic energy spectrum) as a function of layer distance into the metal. Prominent surface bands and surface resonances are identified and their dispersions in k space examined. A detailed description of these states and their relation to orbitals constructed from atomic wave functions is also presented. In addition, for the purpose of analyzing and illustrating surface states, a calculation of the projection of the Nb bulk band structure onto the (001) surface is performed.

Previous calculations[2,6] on the electronic properties of transition-metal surfaces can be roughly divided into the following three general categories: (i) Green's-function calculations[7] of the density of states of semi-infinite crystals using a d-function tight-binding Hamiltonian (i.e., neglecting the effects of sp-d hybridization); (ii) band calculations on semi-infinite crystals by matching wave functions across a potential barrier constructed to represent the surface[8]; and (iii) band calculations on thin films using multiple scattering, tight-binding, or orthogonalized-plane-wave methods.[9]

While the above calculations have provided useful information about band narrowing at the surface and some properties of surface states, the information obtainable from them is somewhat restricted because of the simple models used. Some of the limitations of these calculations are, as mentioned before, none of these calculations are fully self-consistent; tight-binding calculations usually involve a limited basis and therefore some important effects of dehybridization of orbitals at the surface may be neglected; and Green's-function calculations provide only information about the surface density of states without giving individual surface bands and their k-space behavior. To avoid these shortcomings, full band calculations using a relatively complete set of basis functions and performed in a self-consistent fashion are needed. The present work represents a first attempt in this direction.

The remainder of this paper is organized as follows: In Sec. II the methods of calculation are discussed. In Sec. III the results for the electronic structure of the Nb (001) surface are presented together with the projected band structure of bulk Nb on the (001) surface. And in the final Sec. IV a summary and some discussion are presented.

II. METHODS OF CALCULATION

In an earlier paper,[10] referred to hereafter as I, we have shown that, with the inclusion of a nonlocal l-dependent potential, the pseudopotential method can be extended to calculate the electronic structure of bulk Nb. The calculations were performed self-consistently using a Nb^{5+} ionic core pseudopotential determined from atomic spectra. In the present study of the Nb (001) surface, we have used the same Nb^{5+} core potential. The theoretical methods employed are therefore similar to those developed by the present authors for the case of semiconductor surfaces[4,11] except for the additional feature of a nonlocal potential.

A. Projected band structure (PBS)

Since *bona fide* surface states can only occur in the gaps of the projected bulk part of the two-dimensional (2D) band structure,[12] a knowledge of the projected band structure of the three-dimensional (3D) bulk crystal on a crystal face will be extremely helpful in analyzing surface states on that surface. For this reason we have projected the bulk band structure of Nb on the (001) surface using a method similar to that described in Ref. 13 by Caruthers and Kleinman.

For the (001) face of the bcc lattice, the surface lattice vectors are $\vec{a} = a_c \hat{x}$, $\vec{b} = a_c \hat{y}$, where a_c is the the bcc cubic lattice constant and $\hat{x}$, $\hat{y}$, $\hat{z}$ are the usual cubic unit vectors. The 2D Brillouin zone

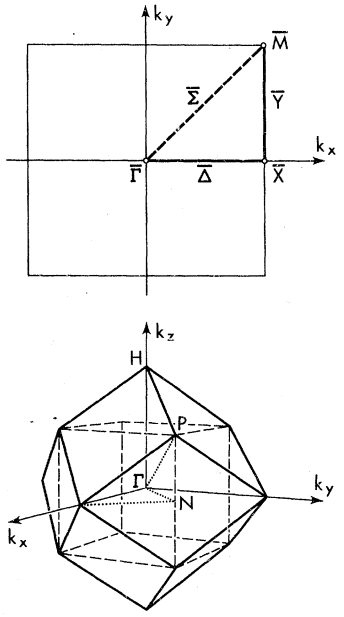

FIG. 1. Brillouin zone for the two-dimensional square lattice and the three-dimensional bcc lattice.

(BZ) for this surface unit cell is then a square (Fig. 1 top) with primitive reciprocal lattice vectors $\vec{K}_x = (2\pi/a_c)\hat{x}$ and $\vec{K}_y = (2\pi/a_c)\hat{y}$. To obtain the PBS, we construct the smallest 3D unit cell of the bcc lattice which is compatible with the 2D surface unit cell and determine the 3D band structure of Nb according to this new unit cell. The allowed energies at a point $\vec{k}_\parallel = (k_x, k_y)$ in the 2D BZ are then the energy eigenvalues at all the points $(\vec{k}_\parallel, k_z)$ such that $-\frac{1}{2}K_z \leq k_z \leq \frac{1}{2}K_z$, where K_z is the primitive reciprocal lattice vector along the $\hat{z}$ direction for the new 3D unit cell.

In the present case, the new unit cell is just the bcc cubic cell and the new BZ is a cube inscribed in the standard BZ (Fig. 1 bottom). The band structure $E_n(\vec{k})$ for the new cell can be easily obtained by folding back the eigenvalues in the standard BZ into the new zone. For this purpose we have used the band structure calculated in I. The PBS for the (001) surface of NB was obtained from the eigenvalues of 285 $\vec{k}$ points in the irreducible part ($\frac{1}{48}$) of the standard BZ. This mesh of $\vec{k}$ points is found to be sufficiently fine to give an accurate determination of the gaps in the PBS of Nb.

B. Self-consistent surface calculations

The method employed here for the calculation of the Nb (001) surface consists of using a thin slab of the Nb crystal to simulate two noninteracting surfaces and repeating the slabs to form a superlattice. The electronic structure is computed in a self-consistent fashion using pseudopotentials. The electronic properties of a single surface are then extracted from the repeated system. This method has been applied successfully to the calculations of a number of local configurations (surfaces,[11] interfaces,[4,14] and vacancies[15]) in simple metals and semiconductors. Since the method has been discussed at length in Refs. 11 and 14, we shall only briefly describe it here.

Some of the desirable features of the present method over existing calculations on transition metal surfaces include: (i) With the introduction of periodicity along the direction perpendicular to the surface, standard pseudopotential techniques in bulk calculations can be used and many of their advantages retained. For example, the electronic wave functions are expanded in simple plane waves eliminating some of the restrictions on the electron wave functions usually associated with limited basis sets. (ii) Self-consistency in the screening potential is required to allow for the correct electronic screening near the surface region. This is achieved by a self-consistent-field procedure with the exchange effects included via a local exchange potential. As in the case of simple metal

and semiconductor surfaces, it has been shown in previous calculations[16] that self-consistency is also very important for transition-metal surfaces.

In the present study, a nine layer slab of Nb with the ideal (001) surfaces exposed to both sides is used to simulate the two noninteracting surfaces. A superlattice is constructed by repeating the slabs with a slab-slab separation equivalent to six atomic layers of Nb. The energy eigenvalues and electron wave functions are calculated from the pseudopotential Hamiltonian

$$H = p^2/2m + V_{ps} + V_H + V_x \,, \tag{1}$$

where V_{ps} is a superposition of Nb^{5+} ionic pseudopotentials

$$V_{ps}(\vec{r}) = \sum_{\vec{R}_n} V_{ion}(\vec{r} - \vec{R}_n) \,. \tag{2}$$

V_H is the Hartree screening potential and V_x is the exchange potential.

For the ionic potentials, we have used the same potential as in I which is an l-dependent nonlocal pseudopotential of the form

$$V_{ion}(\vec{r}) = \sum_{l=0}^{2} V_l(\vec{r}) P_l \,, \tag{3}$$

where the P_l are projection operators for the various angular components of the electron wave function. The nonlocal nature of this potential accounts for the differences in the repulsive potentials that each angular momentum component of the Nb conduction-electron wave function sees as a result of core orthogonalization.[17] The potentials V_s, V_p, V_d were obtained by fitting the spectroscopic term values of the Nb^{4+} ion (i.e., the Nb^{5+} plus one electron system)[18] and they are depicted in Fig. 2. When used in self-consistent atomic and bulk band structure calculations, this Nb^{5+} ionic pseudopotential has yielded results in good agreement with experimental data and with other calculations. (See I.)

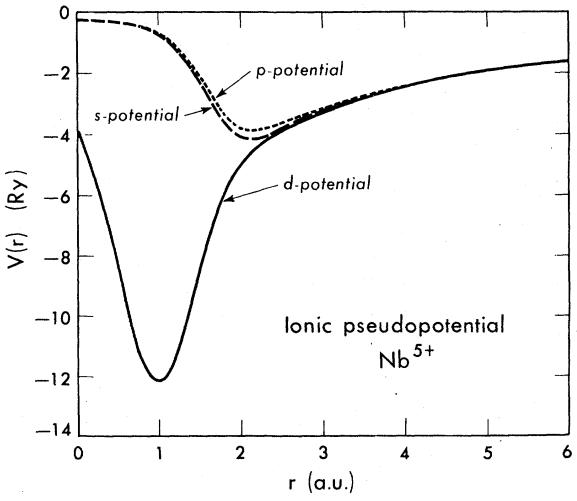

FIG. 2. Nb^{5+} ionic pseudopotentials. V_s, V_p, and V_d plotted as a function of r.

In our self-consistent scheme, the ionic pseudopotential is screened with the Hartree and exchange screening potentials obtained from the pseudocharge density $\rho(\vec{r})$ by

$$\nabla^2 V_H(\vec{r}) = -4\pi e^2 \rho(\vec{r}) \tag{4}$$

and

$$V_x(\vec{r}) = -3\alpha e^2 (3/8\pi)^{1/3} \rho^{1/3}(\vec{r}) \,, \tag{5}$$

where α, the Slater exchange parameter, is chosen to be 0.80.[19] The self-consistent loop is started by approximating the potential terms $V_{ps} + V_H + V_x$ in Eq. (1) by a potential constructed from a superposition of the self-consistently screened atomic pseudopotentials. With this starting Hamiltonian, the valence charge density is calculated from the occupied states and the screening potentials V_H and V_x are derived. The new V_H and V_x are then substituted back into the Hamiltonian for the next iteration. The process is repeated until self-consistency in the screening potentials is reached.

To obtain sufficient convergence for the charge-density calculation, we used the same convergence criteria as in I where plane waves with a maximum reciprocal lattice vector corresponding to an energy of 10.2 Ry were used in the basis set. This led to approximately 1000 plane waves in the expansion of the electronic wave functions; an additional 1000 plane waves were treated by second-order perturbation techniques.[17] Since both $V_H \sim \rho(G)/G^2$ and $V_x \sim \rho^{1/3}(G)$ are short range in $\vec{q}$ space, it does not make a significant difference whether the second group of plane waves is used or not in the self-consistency. We have chosen not to include these in the present calculations. In addition, since the central plane of the slab is a reflection plane, the Hamiltonian was reduced to two ~500×500 matrices using the techniques of symmetrized plane waves. Because of the large matrix size, the self-consistent calculations were based on a three special-point scheme.[20] The three $\vec{k}$ points used were $(\frac{1}{8},\frac{1}{8})$, $(\frac{3}{8},\frac{3}{8})$, $(\frac{3}{8},\frac{1}{8})$ in units of $2\pi/a_c$ with a weighting factor of $\frac{1}{4}$ for the first two points and a weighting factor of $\frac{1}{2}$ for the third point. However, for the final self-consistent potential, a regular mesh of 15 $\vec{k}$ points in the irreducible part ($\frac{1}{8}$) of the 2D square Brillouin zone has been included.

With the results at the 15 $\vec{k}$ points, we obtained the self-consistent valence charge density, the

local density of states for the electrons near the surface, and the charge densities for the various surface states and surface resonances. The surface states or resonances were identified by examining the charge density for all eigenvalues below the vacuum level at the 15 $\vec{k}$ points. The local density of states for a given region, Ω_i, in space was evaluated by

$$N_i(E) = \sum_{k_\parallel, n} \int_{\Omega_i} |\psi_{\vec{k}_\parallel, n}(\vec{r})|^2 d^3r\, \delta(E - E_n(\vec{k}_\parallel)) , \qquad (6)$$

where $\vec{k}_\parallel$ is the wave vector parallel to the surface, n is the band index, and $\psi_{\vec{k}_\parallel, n}$ is the electronic wave function. $N_i(E)$, therefore, gives the probability of finding an electron with energy E in the region Ω_i.

III. RESULTS

A. (001) projected band structure

The PBS for the Nb (001) surface is shown in Fig. 3. We have scanned the entire irreducible part of the square zone by examining $\vec{k}$ points along lines parallel to the $\bar{\Sigma}$ line ($\bar{\Gamma}$ to $\bar{M}$) in equal intervals. Each small figure in Fig. 3 shows the PBS along one of such lines. For example, the upper-left corner figure is the PBS along the $\bar{\Sigma}$ line whereas the low-right corner figure corresponds to the one point $\bar{X}$. As seen from the figures there are a number of absolute gaps in the PBS. Symmetry gaps which we will discuss later are not shown in these figures. We note that the absolute gaps tend to be located far away from the zone center $\bar{\Gamma}$ and tend to be the widest away from high-symmetry points.[21]

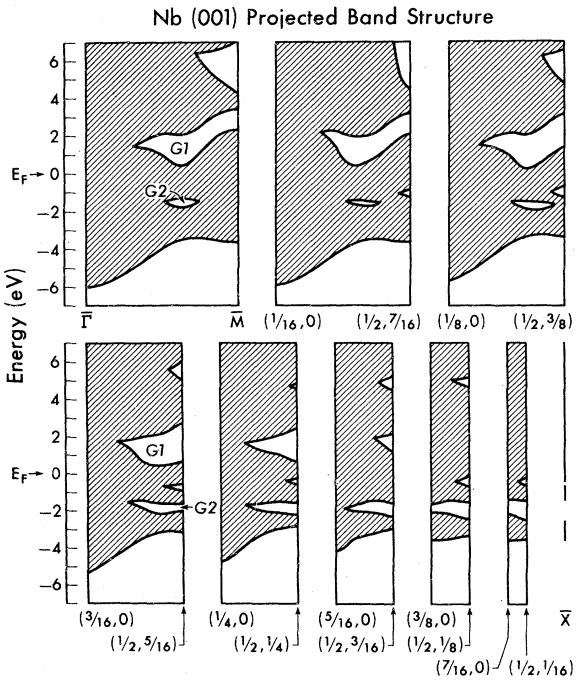

FIG. 3. Projected bulk band structure for the (001) surface of Nb. (See text.)

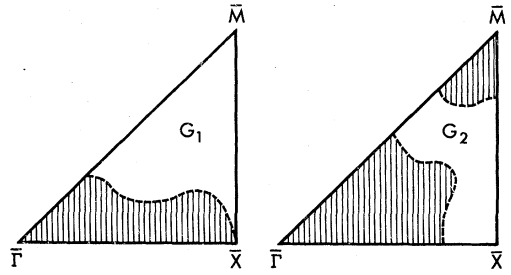

FIG. 4. Extents of the two major absolute gaps in the projected band structure of the Nb (001) surface.

From the PBS one therefore expects most of the surface states to occur away from the zone center and have energies in the wider gaps. Our surface results indeed show that most of the prominent surface states occur in the big gap $G1$ positioned just above the Fermi level E_F between 0 and 3 eV and in the smaller gap $G2$ positioned between −2 and −1 eV. The $\vec{k}$ space extension of these two major gaps in the PBS is shown in Fig. 4. (The unhatched region indicates the existence of the gap.)

B. (001) surface

We shall now proceed to a discussion of the surface results which have been briefly reported re-

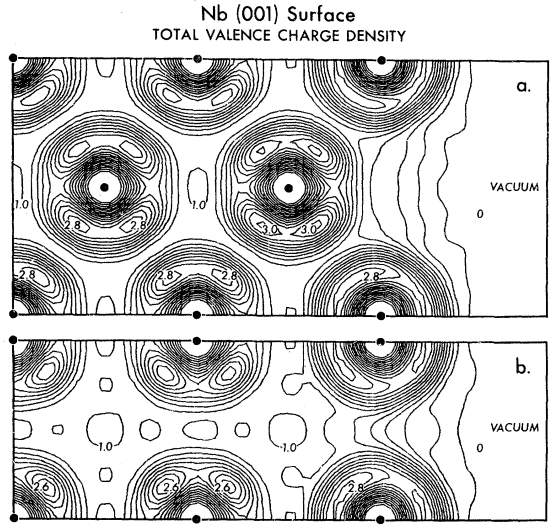

FIG. 5. Total valence charge density of the Nb (001) surface plotted on (a) the (110) plane and (b) the (100) plane. The charge density is normalized to one electron per unit cell.

cently.[22] Figure 5 shows the total, self-consistent valence charge density for the Nb (001) surface. The charge density distribution on the (110) plane is plotted in Fig. 5(a) and that on the (100) plane is plotted in Fig. 5(b). Both planes are perpendicular to the (001) surface. We find that, after only two layers into the bulk, the charge density is virtually identical to the bulk charge density presented in Fig. 4 in I. Some of the noticeable changes in the charge distribution near the surface are: the atoms on the second layer have a slightly higher charge density which can be understood in terms of Friedel oscillations and the charge density at the surface atoms become less directional and more s-like.

The local density of states (LDOS) curves are presented in Fig. 6. The first layer corresponds to the surface layer; the fifth layer at the center of the slab. As stated in Sec. II, fifteen $\vec{k}$ points in the irreducible part of the 2D BZ were used to calculate the LDOS. In addition, to ascertain the surface features, a difference curve obtained by subtracting the LDOS at the center of the slab from the LDOS at the surface is present in Fig. 7. Since most experiments on surfaces are spectroscopic in nature, this LDOS which gives the energy spectrum of the electrons near the surface is one of the most relevant pieces of theoretical information for experimentalists.

As seen from Fig. 6(e) the LDOS away from the surface in layer 5 closely resembles the bulk Nb spectrum given in I. Slight differences occur because of the smaller number of $\vec{k}$ points used and

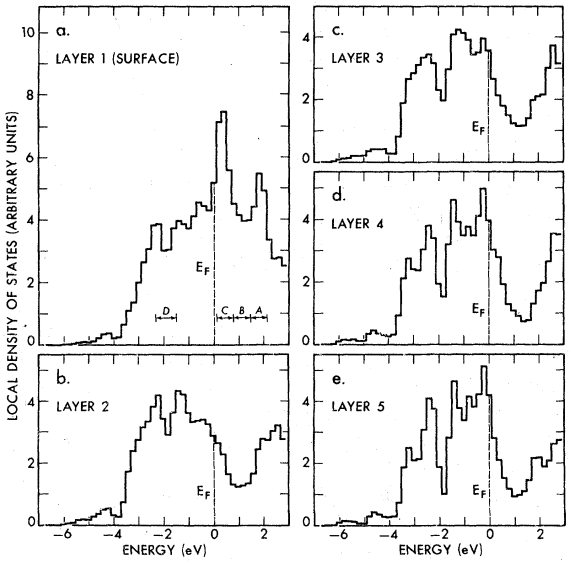

FIG. 6. Calculated local density of states curves for the Nb (001) surface.

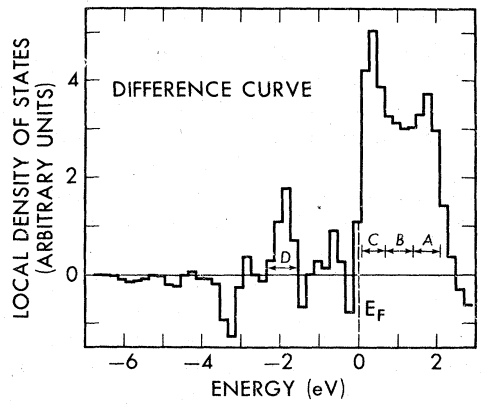

FIG. 7. Difference curve for the local density of states at the Nb (001) surface. (See text.)

also because of some influence of the surfaces. The changes in the LDOS at the surface layer [Fig. 6(a)] are however quite dramatic. These changes are mostly due to surface states (and resonances) and partly due to distortions of the bulk-state wave functions at the surface. In addition, a slight narrowing of the rms width of the LDOS at the surface is observed. In terms of tight-binding arguments,[7] this narrowing arises because of the reduction in neighboring interactions for the surface atoms.

Since Fig. 7 is a difference curve, energy regions where the curve is positive represent an excess in electrons at the surface layer as compared to the bulk. The regions A, B, C, and D shown in Figs. 6 and 7 are therefore regions where most of the prominent surface bands occur. (In the present calculation, we identify surface states and resonances by the localization of their wave functions at the surface layer. Because of the finite slab geometry, some of the weaker surface states or resonances are ignored.) The increase in the density of states at the surface layer in the energy range of 0–2 eV arises mainly from the contributions of three surface bands ($T1$, $T2$, and $T3$). These three surface bands occur in the absolute energy gap $G1$ located just above the Fermi level in the two-dimensional PBS. As seen from Figs. 3 and 4 the $G1$ gap encompasses nearly 70% of the irreducible zone extending from $\bar{M}$ to over $\frac{2}{3}$ of the way to $\bar{\Gamma}$ along the $\bar{\Sigma}$ direction and similarly to nearly touching $\bar{X}$ along the $\bar{Y}$ direction. We find that the existence of these three surface bands in the $G1$ gap is not very sensitive to the potential used. Their dispersion is ~2.5 eV for the $T2$ and $T3$ bands and ~0.4 eV for the $T1$ band. The increase in the density of states at the surface layer in the energy region D, on the other hand, arises from occupied surface states in the smaller

gap $G2$.

Figure 8 shows the various calculated surface bands along the high-symmetry lines in the 2D BZ together with the PBS. Also shown in Fig. 8 are some of the symmetry gaps along the symmetry lines. Symmetry gaps are gaps at high-symmetry points or along symmetry lines in the PBS in which bulk states of a given symmetry are forbidden, but where states of other symmetry may exist. In Fig. 8 vertical crosshatching is used to show the extent of bulk states with $\bar{\Delta}_1$, $\bar{Y}_{1,2}$, and $\bar{\Sigma}_1$ symmetry; horizontal crosshatching is used to show the extent of bulk states with $\bar{\Delta}_2$ and $\bar{\Sigma}_2$ symmetry; and the dash curves are the surface (*bona fide* or strong resonance) bands.

Let us first discuss the surface states in the $G1$ gap. There are four surface bands in this gap. Three of them are the previously mentioned $T1$, $T2$, and $T3$ surface bands. As discussed earlier the $T1$ band is very flat in $\vec{k}$ space, whereas the $T2$ and $T3$ bands are relatively dispersive. The extent of these states encompasses a large fraction of the irreducible Brillouin zone. The fourth band of surface states, on the other hand, is found only at ~3.0 eV in a small region near $\bar{M}$.

As seen from Fig. 8 the $T2$ and $T3$ bands follow each other quite closely in $\vec{k}$ space with a typical energy separation of ~0.5 eV which vanishes near $\bar{M}$. They also yield very similar charge-density distributions. The character[23] of the two bands is for the most part $d_{zx,zy}$ with admixtures of d_{xy} and $d_{x^2-y^2}$, depending on the value of $\vec{k}$. For example, along $\bar{\Sigma}$ the $T2$ band is of $\bar{\Sigma}_1$ symmetry. (see Table I.) Its character is mainly of $d_{z(x+y)}$ with admixture of d_{xy}. The $T3$ band along this direction is however of $\bar{\Sigma}_2$ symmetry and its character is mostly of $d_{z(x-y)}$ with admixture of $d_{x^2-y^2}$. At the point $\bar{M}$ the two bands merge to a twofold-degenerate state with mainly $d_{zx,zy}$ character. The band $T1$, on the other hand, is almost solely of $d_{3z^2-r^2}$ character throughout $\vec{k}$ space. Finally the upper, fourth band which exists only

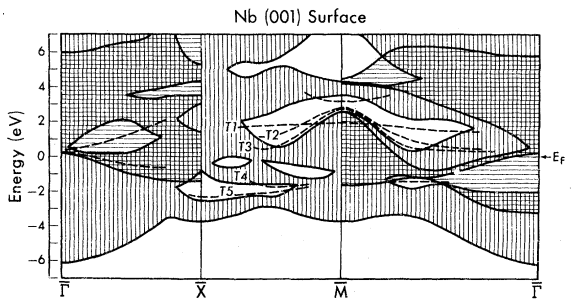

FIG. 8. Surface bands (dashed curves) and the projected band structure for the Nb (001) surface.

TABLE I. Character tables and transformation of d functions in the two-dimensional square Brillouin zone.

$\bar{\Sigma}$	E	M_d	
$\bar{\Sigma}_1$	1	1	$3z^2-r^2, xy, z(x+y)$
$\bar{\Sigma}_2$	1	−1	$x^2-y^2, z(x-y)$
$\bar{\Delta}$	E	M_x	
$\bar{\Delta}_1$	1	1	$3z^2-r^2, x^2-y^2, zx$
$\bar{\Delta}_2$	1	−1	xy, zy
$\bar{Y}$	E	M_y	
$\bar{Y}_1$	1	1	$3z^2-r^2, x^2-y^2, zy$
$\bar{Y}_2$	1	−1	xy, zx

near $\bar{M}$ is mostly of $d_{x^2-y^2}$ character. In terms of spectral weight, the $T2$ and $T3$ states are distributed over regions A, B, and C whereas the $T1$ states are concentrated in region A.

A simple orbital interpretation of the above three prominent surface bands is that the $T2$ and $T3$ surface states are states principally derived from the two bonding orbitals d_{zx} and d_{zy} of the surface atoms. With the formation of the surface, these two bonds are broken and two surface bands split off from the bonding and antibonding part of the spectrum into the $G1$ gap. Similarly the $T1$ states can be thought of as $d_{3z^2-r^2}$ orbitals which split off from the nonbonding part of the spectrum and move down into the $G1$ gap to form one surface band. Of course the situation is much more complex in detail than the above picture. This simple interpretation however does give a clear physical explanation for the behavior of the $T1$, $T2$, and $T3$ states.

There are other surface states near the Fermi level. For example, at $\bar{\Gamma}$, a surface state of $d_{3z^2-r^2}$ character is found in a $\bar{\Gamma}_1$ symmetry gap at 0.2 eV (not shown in Fig. 8). Also found near E_F is an unoccupied surface band in a $\bar{\Delta}_1$ symmetry gap in the PBS along the $\bar{\Delta}$ direction and, just below this $\bar{\Delta}_1$ gap, an occupied band of strong surface resonances. Both of these bands are shown in Fig. 8 but unlabeled. The two bands merge and become weak surface resonances at $\bar{\Gamma}$. Since the state at $\bar{\Gamma}$ and those in the above two bands are well defined surface states only at their perspective symmetry points, they do not contribute much to the LDOS or the total charge density.

The charge-density distributions for states in the regions A, B, and C are shown in Fig. 9. These plots included contributions from both bulk and surface states. As expected from the LDOS, the charges for all three regions are highly local-

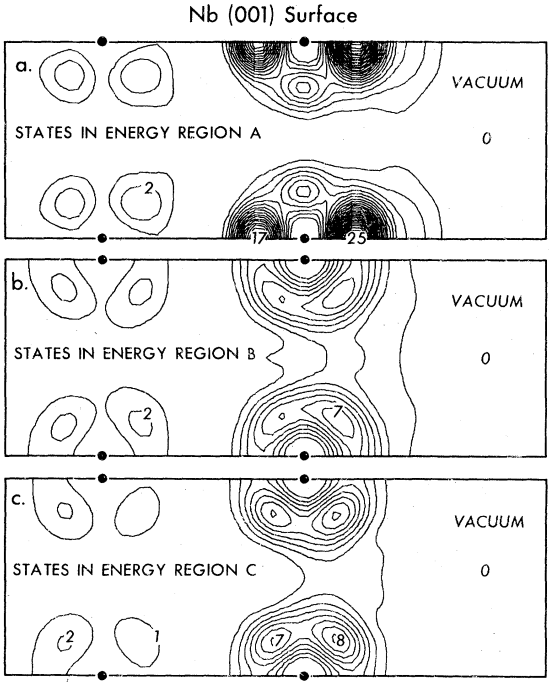

FIG. 9. Charge-density contour plots for the three energy regions (a) region A, (b) region B, (c) region C. (See text.) The charge density for each region is normalized to 1 electron per unit cell and is plotted for a (100) plane cutting the Nb (001) surface.

ized on the first layer, indicating that states in these regions are essentially composed of surface states. Since $T1$ states are dominant in region A, the charge-density plot for this region shows a strong charge lobe about the surface atom protruding into the vacuum region along the z direction perpendicular to the (001) surface. Although it cannot be seen from the plot, the charge density is completely symmetric about the z axis, giving the charge distribution a striking $d_{3z^2-r^2}$ character. In contrast, the charge densities for regions B and C have their maxima protruding into the vacuum region at a 45° angle with respect to the normal; they are nearly symmetric with respect to the z axis. Therefore they are mostly of $d_{zx,zy}$ character with some admixture of d_{xy} and $d_{x^2-y^2}$ character reflecting the fact that the states in region B and C are mostly $T2$ and $T3$ states. From Fig. 9, one can also see the reason for the rather large dispersion for the $T2$ and $T3$ states. The charge densities for these states overlap quite strongly between neighboring surface atoms whereas there is virtually no overlap of charges for the $T1$ states.

Below the Fermi level, two occupied surface bands ($T4$ and $T5$) are found in the energy region D. Similar to the $T1$, $T2$, and $T3$ states, these two bands occur in an absolute gap, the $G2$ gap, in the PBS (Fig. 8). But, unlike the former states, their charge-density distributions are not dangling-bond-like. The $\vec{k}$-space extension of the $G2$ gap is shown in Fig. 4 which consists of a strip extending from midway along the $\overline{\Sigma}$ line to the point $\overline{X}$. An examination of the charge distribution of these states indicated that states in the upper $T4$ band are primarily d_{xy}-like, whereas states in the lower $T5$ band are primarily $d_{x^2-y^2}$-like. However, the character of these states does change significantly over different parts of $\vec{k}$ space. In some regions of $\vec{k}$ space the concentration of charge is shifted from the first (surface) layer to the second layer.

To illustrate some of the characteristics of the *individual* surface states, we have plotted the charge density distributions for the five surface states at the point $\vec{k} = (\frac{3}{8}, \frac{1}{4})2\pi/a_c$. This $\vec{k}$ point was chosen for the reasons that all five surface bands $T1$–$T5$ extend to this point and that it is a general point in the 2D BZ. Figure 10 shows the charge-density distribution for the $T1$ state at $E = 1.6$ eV. The charge distribution on the surface atom is as mentioned before $d_{3z^2-r^2}$-like and has virtually no overlap with the charge from nearby surface atoms. Figure 11 shows the charge density distribution for the $T2$ state at $E = 0.8$ eV. Comparing the charge distribution on the (110) plane [Fig. 11(a)] with that on the (100) plane [Fig. 11(b)], we see that the charge distribution on the surface atom is of $d_{zx,zy}$ character with an admixture of d_{xy} character. Overlap of charges along the [010]

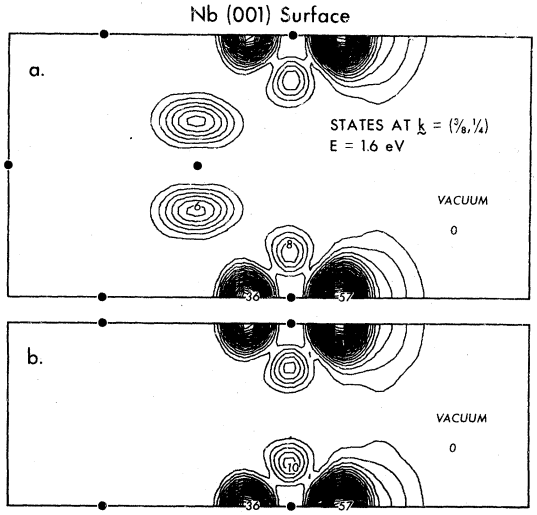

FIG. 10. Charge density distribution of a $T1$ surface state at $\vec{k} = (\frac{3}{8}, \frac{1}{4})2\pi/a_c$ at $E = 1.6$ eV plotted on (a) the (110) plane and (b) the (100) plane. The charge density is normalized to 1 electron per unit cell.

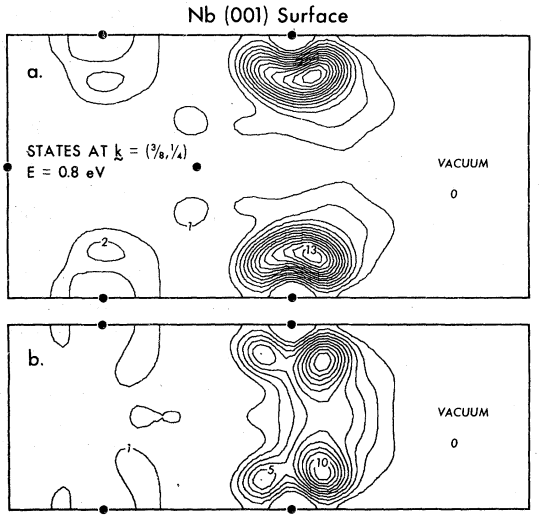

FIG. 11. Charge-density contour plot of a $T2$ surface state at $\vec{k}=(\frac{3}{8},\frac{1}{4})2\pi/a_c$ at $E=0.8$ eV. Plotting planes and normalization are the same as in Fig. 10.

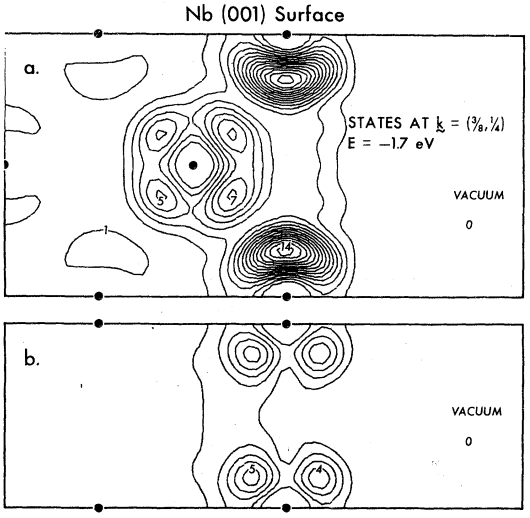

FIG. 13. Charge-density contour plot of a $T4$ surface state at $\vec{k}=(\frac{3}{8},\frac{1}{4})2\pi/a_c$ at $E=-1.7$ eV. See Fig. 10 for plotting planes and normalization.

direction is considerable which is consistent with the large dispersion of the $T2$ band.

Figure 12 shows the charge-density distribution for the $T3$ state at $E=0.4$ eV. The charge distribution is again $d_{zx,zy}$-like. But unlike the $T2$ state, it has an admixture of the $d_{x^2-y^2}$ charge distribution. Again the overlap of charges along the (010) direction is appreciable. Figure 13 shows the charge density distribution for the occupied $T4$ state at $E=-1.7$ eV. The charge density for this state is not as highly localized on the surface atoms as the states in the $G1$ gap. The charge extends into the second layer and is mostly of d_{xy} character with a small admixture of $d_{xz,zy}$ character. Finally, the charge-density distribution for the state $T5$ at $E=-2.0$ eV is presented in Fig. 14. The charge is localized on the second-layer atoms, but extends quite far into the slab.

Finally, a parameter which is closely related to the surface properties and can be obtained directly from our calculations is the work function. From the final, self-consistent potential in the interslab region, we determined that the vacuum level for our system is at 3.6 eV above the Fermi level. Hence this value is the calculated work function. The latest measured work function is 4.0 eV for the (001) surface of Nb.[24]

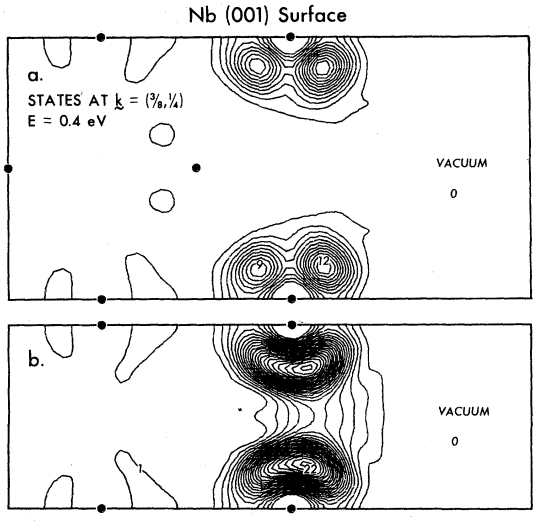

FIG. 12. Charge-density contour plot of a $T3$ surface state at $\vec{k}=(\frac{3}{8},\frac{1}{4})2\pi/a_c$ at $E=0.4$ eV. See Fig. 10 for plotting planes and normalization.

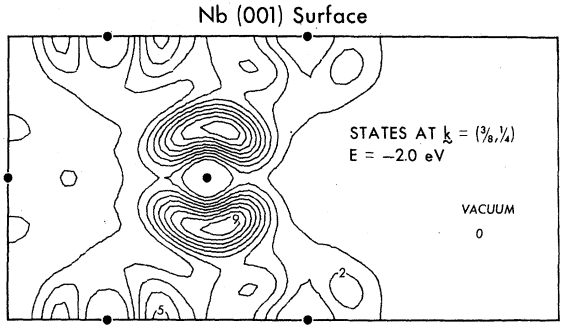

FIG. 14. Charge density distribution of a $T5$ surface state at $\vec{k}=(\frac{3}{8},\frac{1}{4})2\pi/a_c$ at $E=-2.0$ eV plotted on the (110) plane. The charge density is normalized to 1 electron per unit cell.

IV. SUMMARY AND CONCLUSIONS

In summary we have calculated the electronic structure of the (001) ideal surface of niobium using a self-consistent pseudopotential method. Surface states are identified and analyzed throughout the two-dimensional Brillouin zone. When compared to the semiconductor surface states, the surface states on the Nb (001) surface are more complex both in their extent in $\vec{k}$ space and in their charge-density distributions.

Our results also show that most prominent surface bands appear in gaps of the PBS which are located well away from the zone center. Since we do not expect the positions of the gaps in the PBS for the (001) surface of most bcc transition metals to differ much, this situation will most likely occur on other transition-metal surfaces and therefore it is not adequate to analyze the surface properties of transition metals by just examining the $\bar{\Gamma}$ point. Also, since our calculations are nonrelativistic, spin-orbit interactions are not necessary for the existence of the surface states discussed.[25]

Finally, although measurements[26,27] have been done on the (001) surfaces of Mo and W, to our knowledge there is unfortunately no published spectroscopic data on the (001) surface of Nb. The one piece of known experimental information, the work function, appears to agree with the calculated value. It is tempting to make a rigid-band interpretation of our results for Mo and W since the bulk band structures of these materials are very similar. However, because of the change in the Fermi level between materials (i.e., different surface states are occupied), screening at the surface will be likely to significantly alter the energies of the surface states.

Part of this work was done under the auspices of the U. S. Energy Research and Development Administration.

---

†Supported in part by the NSF Grant No. DMR76-20647.
*Work supported by a NSF Fellowship.
‡Present address: Bell Laboratories, Dept. 1111, Murray Hill, N.J. 07974.

[1]See, for example, Phys. Today 28, No. 4 (1975).
[2]B. Feuerbacher and R. F. Wallis, J. Phys. C 9, 169 (1976). This is a review article on photoemission and electron states at clean surfaces. It provides quite an extensive and up-to-date list of references for both theoretical and experimental work on transition-metal surfaces.
[3]J. A. Appelbaum and D. R. Hamann, Rev. Mod. Phys. 48, 479 (1976).
[4]S. G. Louie, J. R. Chelikowsky, and M. L. Cohen, J. Vac. Sci. Technol. 13, 790 (1976).
[5]M. L. Cohen, M. Schlüter, J. R. Chelikowsky, and S. G. Louie, Phys. Rev. B 12, 5575 (1975).
[6]For a survey and additional references see also J. R. Schrieffer and P. Soven, Phys. Today 29, 24 (1975).
[7]R. Haydock, V. Heine, M. J. Kelly, and J. B. Pendry, Phys. Rev. 29, 869 (1972); R. Haydock, V. Heine, and M. J. Kelly, J. Phys. C 5, 2845 (1972); R. Haydock, and M. J. Kelly, Surf. Sci. 38, 139 (1973); J. W. Davenport, T. L. Einstein, and J. R. Schrieffer, Jpn. J. Appl. Phys. Suppl. 2, Part 2 (1974); M. C. Desjonquères and F. Cyrot-Lackmann, J. Phys. (Paris); 36, L45 (1975); and J. Phys. F 5, 1368 (1975).
[8]S. J. Gurman and J. B. Pendry, Phys. Rev. Lett. 31, 637 (1973).
[9]B. R. Cooper, Phys. Rev. Lett. 30, 1316 (1973); R. V. Kasowski, Phys. Rev. Lett. 33, 83 (1974); and Solid State Commun. 17, 179 (1975); E. Caruthers and L. Kleinman, Phys. Rev. Lett. 35, 738 (1975); D. G. Dempsey, L. Kleinman, and E. Caruthers, Phys. Rev. B 12, 2932 (1975); S. J. Gurman, J. Phys. F 5, L194 (1975).
[10]K. M. Ho, S. G. Louie, and M. L. Cohen, Phys. Rev. B 15, 1755 (1977).
[11]M. Schlüter, J. R. Chelikowsky, S. G. Louie, and M. L. Cohen, Phys. Rev. Lett. 34, 1385 (1975); and Phys. Rev. B 12, 4200 (1975); J. R. Chelikowsky and M. L. Cohen, *ibid.* 13, 826 (1976).
[12]V. Heine, Proc. Phys. Soc. 81, 300 (1963).
[13]E. Caruthers and L. Kleinman, Phys. Rev. B 10, 376 (1974).
[14]S. G. Louie and M. L. Cohen, Phys. Rev. Lett. 35, 866 (1975); Phys. Rev. B 13, 2461 (1976).
[15]S. G. Louie, M. Schlüter, J. R. Chelikowsky, and M. L. Cohen, Phys. Rev. B 13, 1654 (1976).
[16]E. Caruthers and L. Kleinman, Phys. Rev. Lett. 35, 738 (1975).
[17]M. L. Cohen and V. Heine, Solid State Phys. 24, 37 (1970).
[18]C. E. Moore, *Atomic Energy Levels*, Natl. Bur. Stand. Circular No. 467 (U.S. GPO, Washington, D.C., 1952), Vol. II.
[19]See Ref. 10 for a discussion of the choice of α.
[20]D. J. Chadi and M. L. Cohen, Phys. Rev. B 8, 5747 (1973); S. L. Cunningham, *ibid.* 10, 4988 (1974).
[21]Similar results have been obtained by Caruthers and Kleinman in Ref. 13 for the projected band structure of bcc iron.
[22]S. G. Louie, K. M. Ho, J. R. Chelikowsky, and M. L. Cohen, Phys. Rev. Lett. 37, 1289 (1976).
[23]In discussing the character of surface states in this paper, we are concerned only with the main *d*-character of the wave functions about the surface atoms.
[24]R. P. Leblanc, B. C. Vanbrugghe, and F. E. Girouard, Can. J. Phys. 52, 1589 (1974).
[25]K. Strum and R. Feder, Solid State Commun. 14, 1317 (1974).
[26]L. W. Swanson and L. C. Crouser, Phys. Rev. Lett. 19, 1179 (1967); E. Al Khouri Nemek, R. C. Cinti, and J. B. Hudson, J. Phys. (Paris) 35, L179 (1974).
[27]E. W. Plummer and J. W. Gadzuk, Phys. Rev. Lett. 25, 1493 (1970); B. Feuerbacher and B. Fitton, *ibid.* 29, 786 (1972); 30, 923 (1973).